ACTA CHROMATOGRAPHICA, NO. 13, 2003

ANALYSIS OF AMYLBENZENE ADSORPTION EQUILIBRIA ON AN RP-18e CHROMATOGRAPHIC COLUMN

M. Gubernak, *W. Zapała*, and *K. Kaczmarski*

Faculty of Chemistry, Rzeszów University of Technology, W. Pola 2 Street, 35-959 Rzeszów, Poland

SUMMARY

The unusual S-shaped isotherm obtained for amylbenzene chromatographed on a reversed-phase high-performance packed column was investigated. A novel adsorption model assuming the possibility of independent adsorption of amylbenzene clusters on the C_{18} chains was proposed. The isotherm model was successfully validated by comparison of breakthrough profiles with those obtained experimentally. The same procedure was used to validate the general rate (GR) and equilibrium-dispersive (ED) models.

INTRODUCTION

Adsorption-based operations are important in large-scale industrial separations and are becoming increasingly sophisticated. One example is the development of preparative chromatography in the pharmaceutical industry. Optimization of these operations requires an accurate model to represent the separation [1]. For economic reasons preparative chromatography must be performed at high concentrations [1], under which conditions the equilibrium is non-linear. The equilibrium isotherms are usually Langmuirian in shape (concave downward) which suggests formation of a simple monolayer. Isotherms can, however, also be S-shaped (concave upward) when multilayer adsorption of molecules is possible.

The literature contains few examples of liquid–solid adsorption systems in which adsorption extends beyond the formation of a simple monolayer [2–5]. Assuming the formation of up to three layers of Troger base isomers has enabled correct prediction of the chromatographic peak profiles of these molecules [5]. S-shaped isotherms are also theoretically possible when lateral interaction between adsorbed molecules has a major

impact on sorption thermodynamics. Such models are, e.g., the Fowler–Guggenheim and Fowler–Guggenheim–Jovanovic isotherms [6,7]. S-shaped isotherms were recently observed for adsorption of butylbenzene and amylbenzene on monolithic silica columns (Chromolith Performance; Merck, Darmstadt, Germany) by Cavazzini et al. [8]. Cavazzini's observations have been confirmed by Gritti et al. [9] on monolithic and on packed columns (Symmetry C_{18} from Waters). A shape similar to that of the amylbenzene isotherm was also observed for butyl benzoate, although with the emphasized non-linearity [9].

The best isotherm model found for the alkylbenzenes was the anti-Langmuir isotherm, whereas for butyl benzoate the liquid–solid state version of the BET isotherm was best [9]. These isotherm models should be treated as a good mathematical approximation of experimental data rather than a description of the physical process. The anti-Langmuir isotherm has no physical interpretation, whereas the BET isotherm is obtained by assuming an infinite number of adsorbed layers of the species. Gritti et al. [9] have showed the BET isotherm to be compatible with the multilayer isotherm for approximately 13 layers; even for such a relatively small number of layers, however, there is insufficient space in the pores to hold this amount of analyte.

Validation of the proposed isotherms was achieved by comparison of theoretical breakthrough curves or peak profiles with those observed experimentally. Agreement between experimental and theoretical breakthrough curves for alkylbenzenes was so poor the authors did not present it [8]. Relatively good agreement was, however, obtained between theoretical and experimental peak profiles of alkylbenzenes for a limited range of concentrations [8]. For butyl benzoate agreement between experimental and theoretical breakthrough curves was better, although to achieve good description of experimental data the number of theoretical plates had to be adjusted to each concentration profile separately [9,10]. Experiment and theory were compared by use of a simple equilibrium-dispersive model or a more complicated POR model [8–10].

Adsorption of alkylbenzenes and butyl benzoate is characterized by a very large adsorption capacity, greater than 100 g dm^{-3}. Such a large adsorption capacity should influence particle porosity. This assumption has been confirmed experimentally for butyl benzoate [10,11]. After introduction of the dependence of particle porosity on fluid concentration to the general rate (GR) model very good agreement was obtained between the GR solution and experimental butyl benzoate breakthrough and peak

profiles on a monolithic column [11]. No additional adjustment of any term of the GR model was needed. Experimental results were not reinterpreted for alkylbenzenes.

Gritti et al. [9] compared adsorption of butylbenzene on a C_{18} chemically bonded silica monolithic column manufactured by Merck (Germany) with that on a Waters column packed with spherical silica particles. Both type of silica were endcapped. The ratio of the equilibrium capacity obtained on the monolithic column to that on the packed column was approximately 1.5, which suggests the novel rod column has a much larger capacity. Probably more interesting, however, would be comparison of monolithic and packed columns manufactured by the same company.

The goal of this work was to investigate amylbenzene adsorption on a Merck LiChrospher RP-18e packed column and to compare the results with experimental data obtained by Cavazzini et al. [8] using a Merck Chromolith Performance column. A second aim was to elaborate a novel isotherm model devoid of BET or anti-Langmuir drawbacks.

THEORY

In this work overloaded elution band profiles were calculated by use of two models of non-linear chromatography, the general rate (GR) and equilibrium-dispersive (ED) models.

The General Rate (GR) Model of Chromatography

Several theoretical models are available to describe the chromatographic process. The most complete and detailed is the GR model, which takes into account all the thermodynamic and kinetic phenomena affecting the separation (adsorption and desorption mechanisms, axial dispersion, and mass-transfer resistance). Complete discussions of this model are widely available [1,12,13]. We present here a short description of the GR model as modified by Piątkowski et al. [11]. In writing the equations of this model, the following assumptions have been made:

- the chromatographic process is isothermal;
- the velocity of the mobile phase is constant and its compressibility is negligible;
- the packing material is porous, spherical, particles of uniform size;
- the concentration gradient in the radial direction of the bed is negligible;

- local equilibrium exists for each component between the pore surface and the stagnant fluid phase in the pores;
- the dispersion coefficient is constant;
- surface diffusion can be ignored; and
- the internal porosity of the adsorbent depends on the concentration in the stationary phase.

With these assumptions, the differential mass balance of each feed component in the mobile phase can be expressed as:

$$\varepsilon_{\mathrm{e}} \frac{\partial C_i}{\partial t} + u \frac{\partial C_i}{\partial z} = \varepsilon_{\mathrm{e}} D_{\mathrm{L}} \frac{\partial^2 C_i}{\partial z^2} - (1-\varepsilon_{\mathrm{e}}) \frac{3}{R_{\mathrm{p}}} k_{\mathrm{ext}} (C_i - C_{\mathrm{p},i}) \tag{1}$$

and the mass balance equation for the stagnant liquid phase within the pores of the particles can be formulated as:

$$\frac{\partial [\varepsilon_{\mathrm{p}}(q) C_{\mathrm{p},i}]}{\partial t} + (1-\varepsilon_{\mathrm{p}}^0) \frac{\partial q_i}{\partial t} = \frac{1}{r^2} \frac{\partial}{\partial r} \left[r^2 \frac{D_{\mathrm{m}} \varepsilon_{\mathrm{p}}(q)}{\gamma} \frac{\partial C_{\mathrm{p},i}}{\partial r} \right] \tag{2}$$

In these equations C_{i} and $C_{\mathrm{p},i}$ are the concentrations of component i in the mobile and the stagnant liquid phases, respectively, q_i is the concentration of component i in the solid phase, z is the distance along the column, r is the distance from the particle center, R_{p} is the particle diameter, ε_{p} is the internal porosity of the particles of the packing material, $\varepsilon_{\mathrm{p}}{}^0$ is the initial value of the internal porosity, u is the superficial velocity, k_{ext} is a external mass transfer coefficient, and γ is the tortuosity factor. In this work the concentration, q, is related to the adsorbent volume so in second term of eq. (2) the initial particle porosity $\varepsilon_{\mathrm{p}}{}^0$ must be used; this is the value of the porosity when the species concentration is zero.

The GR model must be coupled with initial and boundary conditions. We assumed that the concentrations of the feed components in the liquid phase and on the surface of the solid phase are equal to zero at time $t = 0$. As the boundary conditions for eq. (1) we have applied classical Dankwerts equations:

for $t > 0$ and z = 0

$$\begin{aligned} & u_f C'_{f,i} - u(0) C(0) = -\varepsilon_{\mathrm{e}} D_{\mathrm{L}} \frac{\partial C_i(t,0)}{\partial z} \\ & \mathrm{C}'_{f,i} = \mathrm{C}'_{f,i} \text{ for } 0 < t < t_{\mathrm{p}} \\ & \mathrm{C}'_{f,i} = 0 \text{ for } t_{\mathrm{p}} < t \end{aligned} \tag{3}$$

where t_p is the injection time and $C'_{f,i}$ the inlet concentration.

for $t > 0$ and $z = L$ (where L is the column length):

$$\frac{\partial C_i}{\partial z} = 0 \tag{4}$$

The boundary conditions for eq. (2) are:

for $t > 0$ and $r = R_p$

$$\frac{D_m \varepsilon_p(q)}{\gamma} \frac{\partial C_{p,i}}{\partial r} = k_{ext}(C_i - C_{p,i}) \tag{5}$$

and for $t > 0$, at $r = 0$, we have:

$$\frac{\partial C_{p,i}(t,r)}{\partial r} = 0 \tag{6}$$

Equations (1) to (6), together with a suitable isotherm model constitute the GR model.

The Equilibrium-Dispersive (ED) Model

The equilibrium-dispersive model is most often used when mass resistances are small [1]. This model assumes instantaneous equilibrium between the mobile and the stationary phases but finite column efficiency. The contribution of axial dispersion and of resistance to mass transfer to band broadening is taken into account by a contribution to the dispersion coefficient. There is now one mass balance equation only for the mobile phase; it is:

$$\frac{\partial C_i}{\partial t} + \frac{1-\varepsilon_t}{\varepsilon_t} \frac{\partial q_i}{\partial t} + \frac{u}{\varepsilon_t} \frac{\partial C_i}{\partial z} = D_a \frac{\partial^2 C_i}{\partial z^2} \tag{7}$$

where ε_t is the total porosity of the column and the apparent axial dispersion coefficient, D_a, is related to the number of theoretical plates of the column N by eq. (8):

$$D_a = \frac{uL}{2N} \tag{8}$$

In this model we have ignored the dependence of total porosity, ε_t, on surface concentration q. The ED model was coupled with boundary and initial conditions analogous with those for eq. (1).

Numerical Solutions of the GR Model and the ED Model

The ED and GR models were solved by use of a computer program based on an implementation of the method of orthogonal collocation on finite elements [1,14–16]. The set of discretized ordinary differential equations was solved with the Adams–Moulton method, implemented in the VODE procedure [17]. The relative and absolute errors of the numerical calculations were 1×10^{-6} and 1×10^{-8}, respectively.

Adsorption Equilibrium Isotherms

Experimental isotherm data $q = f(C)$ acquired in this paper were fitted to different models of adsorption isotherms for liquid–solid equilibrium. As has already been mentioned the amylbenzene isotherm is S-shaped. Such an isotherm can be successfully approximated by use of the anti-Langmuir isotherm model [8]; because there is no physical interpretation of this model, however, in this work the anti-Langmuir isotherm was not investigated. S-shaped isotherm curvature can, on the other hand, also be achieved when adsorbed molecules interact with each other or when there is a possibility of multilayer formation.

Isotherms with Lateral Interaction Between Adsorbed Species

The Fowler–Guggenheim (FG) Isotherm

This isotherm model [6] assumes ideal adsorption on a set of localized sites with weak interactions between molecules adsorbed on neighboring sites. It assumes also that the interaction energy between two sorbate molecules is so small that the random character of distribution of the sorbate molecules on the adsorbent surface is not significantly altered. For liquid–solid equilibria the FG isotherm is extended empirically and written:

$$KC = \frac{\theta}{1-\theta} e^{-\chi\theta} \tag{9}$$

where χ is an empirical interaction energy parameter between two molecules adsorbed on nearest-neighbor sites and θ is the degree of surface coverage.

The Fowler–Guggenheim–Jovanovic (FGJ) Model

The FGJ model [7] assumes, as before, the occurrence of interactions between molecules adsorbed as a monolayer but is based on the Jovanovic isotherm. The single-component isotherm is represented by the equation:

$$\theta = 1 - e^{-(aCe^{\chi\theta})} \tag{10}$$

where a is a model constant.

The Kiselev Model

This model assumes single-component localized adsorption with specific lateral interactions between all adsorbed molecules in the monolayer [18–20]. The equation of the Kiselev isotherm model is:

$$\frac{\theta}{(1-\theta)\times C} = \frac{K}{\left(1 - K \times K_{\mathrm{a}}(1-\theta)C\right)^2} \tag{11}$$

where $\theta = q/q_{\mathrm{s}}$, K is the equilibrium constant for adsorption of the analyte on an active site, and K_{a} is the association constant.

The Multilayer Isotherms

The BET Isotherm

The multilayer isotherm models can be derived from the equations:

$$K_1 \times C \times (q_{\mathrm{s}} - q_1 - q_2 - q_3 - \ldots - q_n) - \mathrm{q}_1 = 0 \tag{12}$$
$$K_2 \times C \times q_1 - q_2 = 0 \tag{13}$$
$$K_3 \times C \times q_2 - q_3 = 0 \tag{14}$$
$$\ldots\ldots\ldots\ldots\ldots\ldots\ldots\ldots$$
$$K_n \times C \times q_{n-1} - q_n = 0 \tag{15}$$

where the first equation describes the equilibrium between free active centers and adsorbed species and the next equations depict equilibrium between the previous and the next analyte layer. It is generally assumed that

$$K_2 = K_3 = \ldots = K_n = K_{\mathrm{a}}$$

For only two layers the quadratic isotherm model is obtained. When the number of layers is infinite the liquid–solid version [9] of the BET isotherm first proposed in Ref. [21] is obtained:

$$q = q_s \frac{K_1 C}{(1 - K_a C)(1 - K_a C + K_1 C)} \tag{16}$$

The BET isotherm, widely used to describe gas–solid equilibria, proved to be a good approximation of experimental data for butyl benzoate [9]. The physical drawback of this model is the assumption of formation of an infinite number of layers. Gritti et al. [9] have proved that for butyl benzoate the model (eqs 12–15) is compatible with the BET isotherm for approximately 13 layers. There is, however, insufficient space in monolithic mesopores even for such restricted numbers of layers. The diameters of mesopores are only 13 nm, so it seems that the BET isotherm is only a good mathematical approximation of experimental data and has restricted physical meaning.

The Cluster Isotherm

As has already been mentioned the anti-Langmuir isotherm and the BET isotherm are good models for approximation of the S-shaped isotherm; physical interpretation of adsorption process for discussed species is, however, problematic. In this work we have proposed and verified another model. Before formulation of the model it should be noted that the solubility of amylbenzene in the mobile phase used by Cavazzini et al. (80:20, *v*/*v*, methanol–water) [8] is only approximately 10 g dm^{-3}. The maximum surface concentration achieved was approximately 155 g dm^{-3} for a liquid concentration of 8 g dm^{-3}.

Instantaneous equilibrium between adsorbed and desorbed species is usually assumed, but it should be remembered that even under equilibrium conditions large numbers of species molecules are being adsorbed and desorbed with average proportions depending on the equilibrium conditions. It seems possible that, because of fluctuations in the adsorption–desorption process and the extremely high surface concentration, supersaturation can arise leading to formation of clusters of amylbenzene. These clusters can become adsorbed on the adsorbent surface. It was assumed that hypothetical clusters could be adsorbed preferentially by the first adsorbed analyte layer.

With these assumptions the following model, similar to that depicted by eqs (12)–(15), can be formulated:

$$K_1 \times C \times (q_s - q_1 - q_2 - q_3 - \ldots - q_n) - q_1 = 0 \quad (17)$$
$$K_2 \times C \times q_1 - q_2 = 0 \quad (18)$$
$$K_3 \times C \times C \times q_1 - q_3 = 0 \quad (19)$$
$$\ldots\ldots\ldots\ldots\ldots\ldots\ldots\ldots\ldots$$
$$K_n \times C^{n-1} \times q_1 - q_n = 0 \quad (20)$$

Equation (17) is identical with eq. (12). Equations (18)–(20) depict equilibrium between hypothetical clusters and the first analyte layer. The development of eqs (18)–(20) requires explanation. Local supersaturation should lead to formation of clusters of analyte. In equilibrium between single amylbenzene molecules and the clusters the following relationship is valid:

$$K_{c,n-1} \times C^{n-1} - C_{n-1} = 0 \quad (i)$$

where $K_{c,n-1}$ is the equilibrium constant for cluster formation and C_{n-1} is the concentration of clusters containing n–1 molecules.

According to our assumption, on other hand, the clusters interact with amylbenzene molecule adsorbed on the C_{18} ligands. The equilibrium of the adsorption–desorption process is described by the equation:

$$K_{a,n-1} \times C_{n-1} \times q_1 - q_n = 0 \quad (ii)$$

where $K_{a,n-1}$ is the adsorption equilibrium constant. Substituting eq. (i) into eq. (ii) gives the relationship:

$$K_{a,n-1} \times K_{c,n-1} \times C^{n-1} \times q_1 - q_n = 0 \quad (iii)$$

Equation (iii) is consistent with eq. (20) where $K_n = K_{a,n-1} \times K_{c,n-1}$ is the apparent adsorption equilibrium constant.

Solution of eqs (17)–(20) gives:

$$q_1 = \frac{q_s \times K_1 \times C}{D} \quad (21)$$
$$q_2 = \frac{q_s \times K_1 \times K_2 \times C^2}{D} \quad (22)$$
$$\ldots\ldots\ldots\ldots\ldots\ldots\ldots\ldots\ldots\ldots..$$
$$q_n = \frac{q_s \times K_1 \times K_n \times C^n}{D} \quad (23)$$

where:

$$D = 1 + K_1 \times C + K_1 \times K_2 \times C^2 + \ldots + K_1 \times K_n \times C^n = 0 \quad (24)$$

The total concentration of adsorbed molecules is:

$$q = q_1 + 2 \times q_2 + \ldots + n \times q_n \quad (25)$$

In the following text the model described by eqs (21)–(25) is called the cluster isotherm model.

EXPERIMENTAL

Chemicals

The mobile phase used in this work was 80:20 (*v*/*v*) methanol–water. The analyte was amylbenzene. Uracil was used for measurement of column dead-time. All chemicals were purchased from Merck (Darmstadt, Germany). The mobile phase flow rate was 1.0 cm^3 min^{-1} in all experiments.

Column

All experiments were performed with a 125 mm × 4.0 mm i.d., 5-μm particle, LiChroCart, LiChrospher 100, RP-18e column (Merck, Darmstadt, Germany). The column dead time, determined as the retention time of uracil, was 0.939 min. The dead time calculated from the total porosity was $\varepsilon_t = 0.598$.

Apparatus

Chromatography was performed with a Merck–Hitachi LaChrom model chromatograph assembled from an L-7100 LaChrom pump, an L-7455 DAD LaChrom detector, a D-7000 LaChrom interface, an L-7350 column oven, and an L-7612 solvent degasser. Absorbance was measured at 272.1 nm. All measurements were performed at a constant temperature of 24°C. The extra-column dead time was 0.093 min.

RESULTS AND DISCUSSION

Determination of the Isotherm

All the adsorption data used in this work were derived from frontal analysis results by use of the equal area method. The experimental dependence of amount of adsorbed amylbenzene on its concentration in the mobile phase was calculated by use of the equation:

$$q = \frac{V_r(C) - V_0(C)}{V_a} \cdot C = \frac{V_r(C) - V_0(C)}{V_0(C)} \cdot \frac{V_0(C)}{V_a} \cdot C \tag{26}$$

where $V_0(C)$ is the hold-up volume, measured by recording the retention time of an unretained compound at the plateau concentration, V_a is the volume of stationary phase, V_r is the retention volume of the breakthrough curve, q is the concentration in the solid phase at equilibrium with the plateau concentration in the fluid phase.

After simple mathematical simplification, eq. (26) can be written:

$$q = \frac{t_r(C) - t_0(C)}{t_0(C)} \cdot \frac{\varepsilon_t(C)}{(1 - \varepsilon_t^0)} \cdot C \tag{27}$$

where $t_0(C)$ is the hold-up time, $\varepsilon_t(C)$ the total porosity, which depends on the plateau concentration, C, and ε_t^0 is the total porosity when the column is equilibrated with the pure mobile phase (for a plateau concentration equal to zero).

Finally, the equilibrium concentration of amylbenzene was calculated by use of eq. (27). The equilibrium surface concentration of amylbenzene as a function of its concentration in the mobile phase is presented in Table I. Let us calculate the amount of amylbenzene adsorbed on a

Table I

Dependence of amylbenzene surface concentration on liquid concentration

C	q^*	C	q^*
0.1	1.408	1	14.52
0.2	2.78	2	28.95
0.3	4.17	3	43.89
0.4	5.57	4	59.44
0.5	7.06	5	75.27
0.6	8.46	6	91.90
0.75	9.83	7	110.46
0.9	12.84	8	134.17

square meter of pore surface in a packed column. For the fluid phase the concentration is 8 g dm^{-3}; the surface concentration of adsorbed analyte in our experiment was 134 g dm^{-3}. The molar mass of amylbenzene is 148.25 g mol^{-1} and the surface area is 350 m^2 g^{-1}. Assuming a density of 2.2 g cm^{-3} for silica this gives the amount of adsorbed amylbenzene as

0.134/148.25/2.2/350 = 1.17 μmol m^{-2}. The density of the bonded C_{18} chains is 4.09 μmol m^{-2}, which is equivalent to approximately 28 molecules of amylbenzene adsorbed for 100 C_{18} chains.

The same calculation for a monolithic column gives the following results. The surface area of a monolithic column is 300 m^2 g^{-1} and the solid phase concentration was 155 g dm^{-3} [8] which gives 0.155/148.25/2.2/300 = 1.58 μmol m^{-2}. The density of bonded C_{18} chains is 3.6 μmol m^{-2}, so approximately 44 molecules are adsorbed for 100 C_{18} chains. In this calculation we ignored the small error associated with calculation of surface concentration by Cavazzini et al. [8] who neglected changes of particle porosity.

This result confirms the conclusion from previous work that adsorption is more effective in monolithic columns.

An interesting result is obtained after calculation of the density of adsorbed amylbenzene molecules. For a concentration of amylbenzene equal to $q(C = 8)$ = 134 g dm^{-3} the particle porosity, ε_p, is 0.271 whereas for $q(C = 0) = 0$ particle porosity, ε_p^0, is 0.362. The change of porosity is $\Delta\varepsilon = 0.091$. Assuming amylbenzene does not penetrate the alkyl chains, the density of the adsorbed layer for $q(C = 8)$ is:

$$\rho = \frac{q \times (1 - \varepsilon_p^0)}{\Delta\varepsilon} = \frac{q^*(1 - \varepsilon_t^0)}{\varepsilon_t^0 - \varepsilon_t} = 0.94 \text{ g m}^{-3} \tag{28}$$

The density obtained is slightly higher than the density of liquid amylbenzene, which is 0.86 g cm^{-3}. This suggests that weak penetration of C_{18} chains by amylbenzene molecules is possible, although generally the analyte seems to be adsorbed on the surface of the C_{18} chains.

Verification of the Isotherm Models

From the results obtained above it seems there is enough space on the surface of the C_{18} chains for single-layer adsorption of evenly distributed amylbenzene molecules. The S-shaped isotherm suggests there should be lateral interaction between adsorbed molecules, however. To validate this hypothesis, the Fowler–Guggenheim, Fowler–Guggenheim–Jovanovic, and Kiselev models were first compared with experimental data. Unfortunately, agreement between experimental and theoretical isotherms was poor or the value obtained for saturation capacity, q_s, was enormously large.

In a second step the cluster isotherm and, for comparative reasons, the BET isotherm were tested. The value of the product $q_s \times K_1$ was calcu-

lated from the retention time of peak profiles obtained at very low concentrations. For very low concentrations the cluster and BET isotherms converge to a linear isotherm $q = q_s \times K_1 \times C = H \times C$. The calculated Henry constant, H, was 13.92. Other terms of the model were derived by minimizing sum of the squares of differences between experimental and theoretical data, by use of the least-squares Marquardt method as modified by Fletcher [22]. The values of the terms are presented in Table II.

Table II

Isotherm terms

Terms	Model:		
	BET	Cluster	Polynomial
K_1	0.0923	0.0297	13.80
K_2	0.0482	0.0203	0.623
K_3	–	0	–0.152
K_4	–	1.10×10^{-4}	0.0151
SSD*	0.578	0.582	0.184

*Sum of squares of differences between experimental and theoretical data

The approximations of the experimental data obtained by use of the BET and cluster isotherms were comparable. In contradiction with the infinite number of layers claimed by the BET isotherm, up to three molecules only in a cluster were required by the cluster model approximation. The sum of the squares of differences (SSD) between experimental and theoretical data was nearly identical for both isotherms.

The best agreement between experimental and theoretical isotherms was obtained by application of a simple polynomial model:

$$q = K_1 \times C + K_2 \times C^2 + K_3 \times C^3 + K_4 \times C^4 \qquad (29)$$

where K_i have no physical sense and are adjustable terms only. For the simple polynomial model the SSD was less than one third that for the BET or cluster isotherms; as shown in the next section, however, the polynomial isotherm poorly approximates the experimental breakthrough curve profiles for the highest concentrations. Experimental and theoretical isotherms are compared in Fig. 1. The discrepancies between all the lines are so small that on the scale of the figure they overlap.

The saturation capacity calculated for the cluster isotherm is $q_s = 13.92/K_1 = 469$ g dm^{-3}. After calculation similar to that in the section

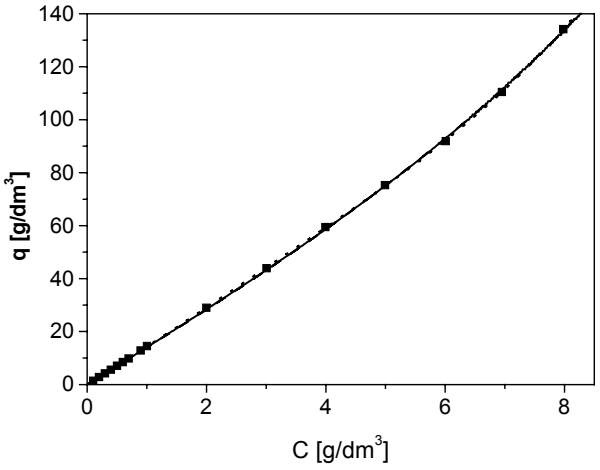

Fig. 1

Comparison of experimental isotherm data for amylbenzene (symbols) with the BET (dashed line), cluster (solid line), and polynomial (dotted line) theoretical isotherms

above we find the density of adsorbed amylbenzene to be 4.27 μmol m^{-2}, very close to the density of the bonded C_{18} chains (4.09 μmol m^{-2}). The saturation capacity obtained from the BET isotherm is 150.8 g dm^{-3}, but it must be remembered that this isotherm assumes an infinite number of layers, so q_s should be regarded as an adjustable term.

Validation of the Isotherm Models

To validate the isotherm models the GR chromatography column model coupled with the cluster, BET, or polynomial isotherms was solved. The values of the terms used in the GR model are listed in Table III. The dispersion coefficient was calculated by use of the Gunn equation [23]. The Wilke–Chang [24] correlation, as extended to mixed solvents by Perkins and Geankopolis [25], was used to calculate the molecular diffusion coefficient of amylbenzene in the mobile phase. The mass-transfer coefficient was calculated from the Wilson and Geankopolis correlation [26]. The tortuosity factor was calculated by use of eq. (30) [1]:

$$\gamma = \frac{\left(2 - \varepsilon_p^0\right)^2}{\varepsilon_p^0} \tag{30}$$

Table III

Values of the terms used in the GR model

Term	Numerical value
Dispersion coefficient, D_L ($cm^2\ min^{-1}$)	0.0032
Molecular diffusion coefficient, D_m ($cm^2\ min^{-1}$)	0.00061
External mass transfer, k_{ext} ($cm\ min^{-1}$)	6.68
Total porosity,* ε_t	0.598
External porosity, ε_e	0.37 – assumed value
Internal porosity, $\varepsilon_p = \frac{\varepsilon_t - \varepsilon_e}{1-\varepsilon_e}$	0.362 – calculated value
Tortuosity factor, γ	7.41

*Value calculated from the retention of unadsorbed uracil

assuming that pore clogging has no effect.

As well as the GR model terms given above, the dependence of particle porosity on surface concentration, $\varepsilon_p = \varepsilon_p(q)$, must be introduced. This dependence was calculated from the relationship between bed porosity, ε_e, total porosity, ε_t, and particle porosity:

$$\varepsilon_p = \frac{\varepsilon_t - \varepsilon_e}{1-\varepsilon_e} \quad . \tag{31}$$

After introducing the experimental relationship between total porosity and mobile phase concentration and the relationship between equilibrium surface concentration and mobile phase concentration into eq. (31), the dependency $\varepsilon_p = \varepsilon_p(q)$ depicted in Fig. 2. was obtained. The functional relationship between ε_p and q was approximated by the equation: $\varepsilon_p = \varepsilon_p^o - 0.000696 \times q = 0.362 - 0.000696 \times q$.

Results from simulations performed with the GR model are compared with experimental data in Figs 3–5. The approximations of experimental data by the cluster and BET models are very similar, so both models can be used. Only the cluster isotherm seems to have physical sense, however. If the polynomial isotherm is used a substantial discrepancy between the shapes of experimental and theoretical breakthrough profiles is observed for high analyte concentrations. Because the polynomial isotherm best approximates the experimental isotherm data this disagreement is a surprise.

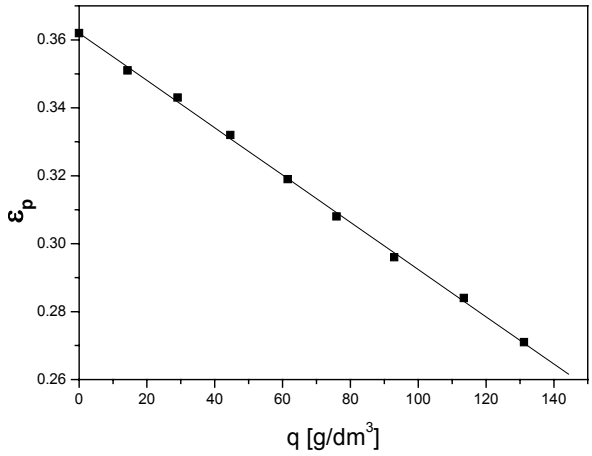

Fig. 2

The dependence of particle porosity on surface concentration

These results confirm that theoretical isotherm models must be validated by comparison with experimental concentration profiles. The discrepancy between simulated and experimental breakthrough profiles proves, moreover, that calculated results are very sensitive even to extremely small differences between theoretical isotherms.

Figures 6–8 illustrate the agreement obtained between the experimental breakthrough profiles and theoretical profiles simulated by use of the GR and ED models. Calculations with the ED model were performed for $N = 6900$ theoretical plates, using the experimental Gaussian peak profile of amylbenzene. The concentration profiles generated by both models are very similar, suggesting that breakthrough shape profiles depend mainly on sorption thermodynamics and that the effects of resistance to mass transfer on outlet concentration profiles are negligible.

CONCLUSIONS

In the work described in this paper the adsorption of amylbenzene on LiChrospher RP-18e was investigated. A novel adsorption model assuming the possibility of independent adsorption of analyte clusters on the C_{18} chains was proposed. In contradiction with the BET isotherm, which assumes formation of an infinite number of analyte layers, the

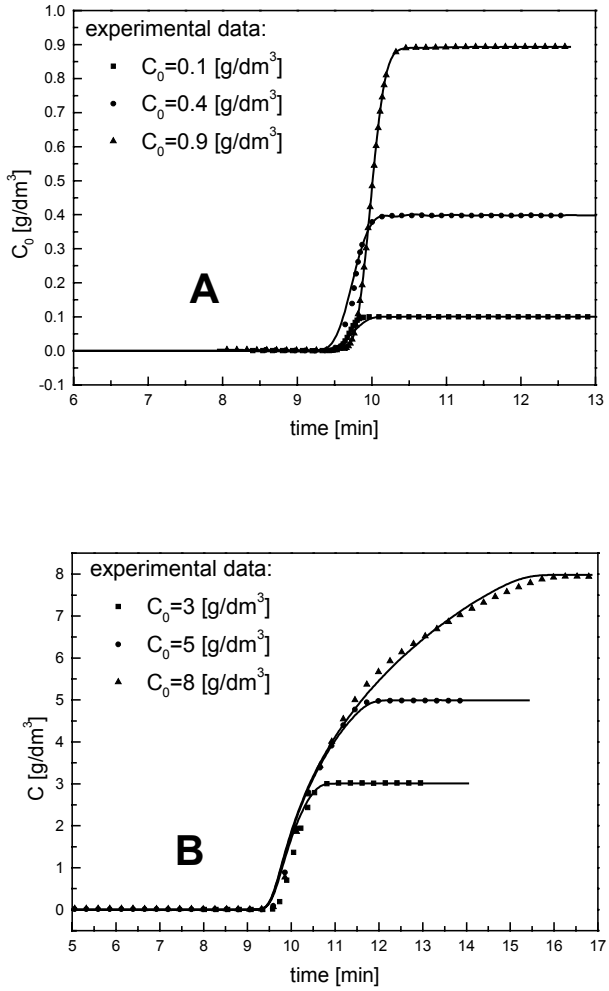

Fig. 3

Comparison of experimental (symbols) and theoretical (solid line) breakthrough profiles for the BET isotherm model: A. low concentration; B. high concentration. Theoretical calculations were performed with the GR model

novel isotherm predicts interactions of up to four molecules only with one active site, which is more physically probable.

Very good agreement was obtained between experimental breakthrough profiles and those calculated by use of the GR model.

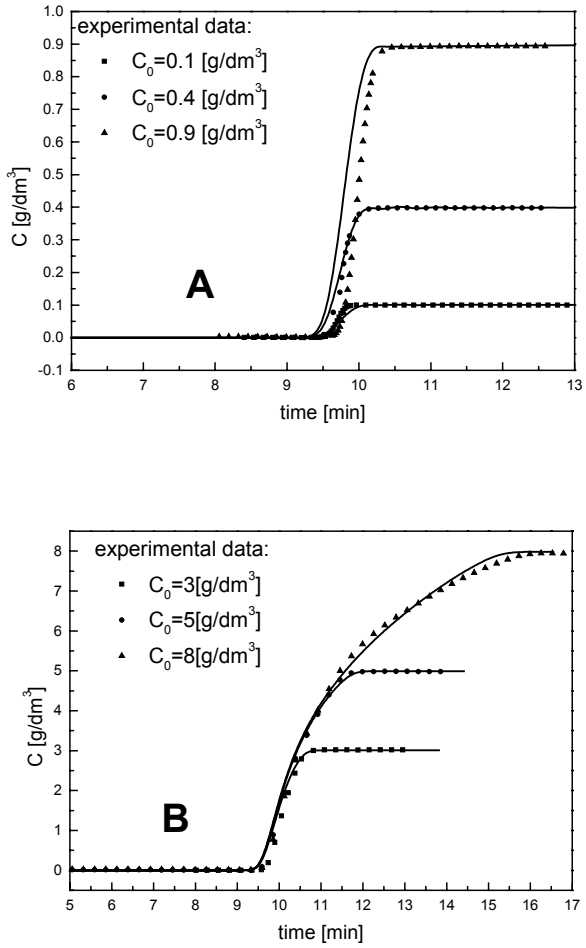

Fig. 4

Comparison of experimental (symbols) and theoretical (solid line) breakthrough profiles for the cluster isotherm model: A. low concentration; B. high concentration. Theoretical calculations were performed with the GR model

The similar simulated breakthrough profiles obtained by use of the GR and ED models imply that resistance to mass transfer is negligible in the chromatographic process investigated.

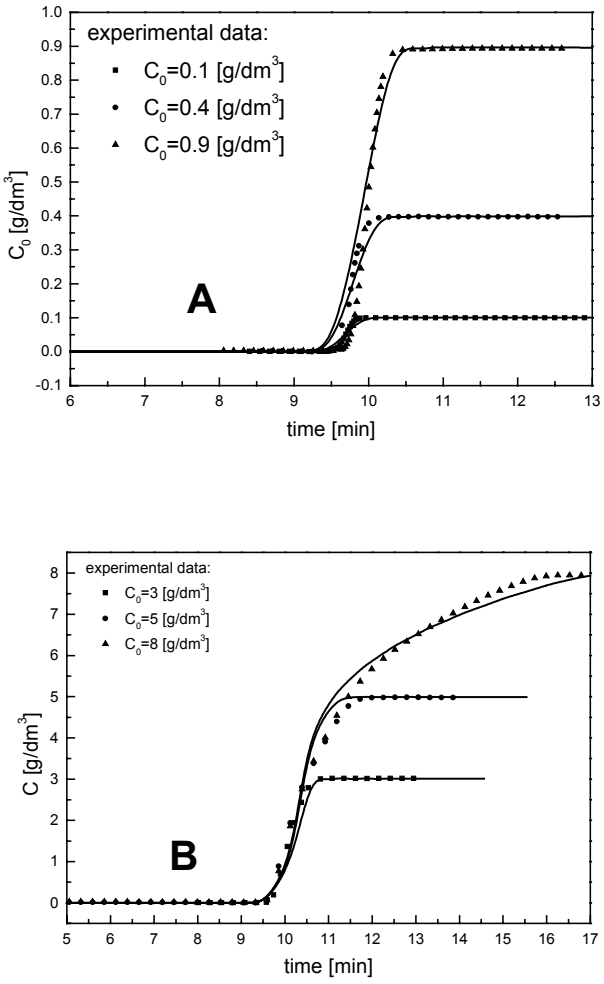

Fig. 5

Comparison of experimental (symbols) and theoretical (solid line) breakthrough profiles for the polynomial isotherm model: A. low concentration; B. high concentration. Theoretical calculations were performed with the GR model

ACKNOWLEDGEMENT

This work was supported by Grant 4 T09C 006 23 of the Polish State Committee for Scientific Research.

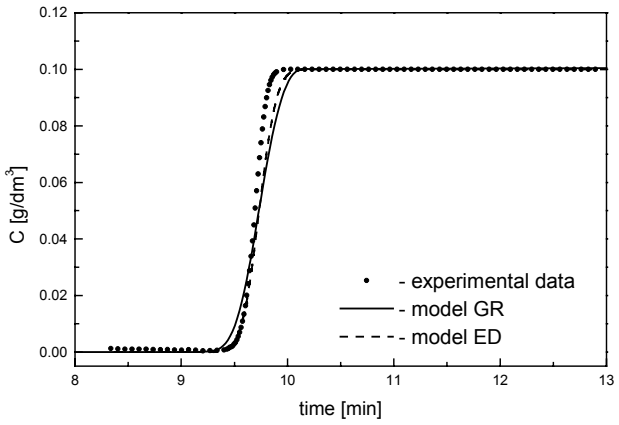

Fig. 6

Comparison of experimental data with theoretical breakthrough profiles calculated by use of the GR and ED models. The inlet concentration of amylbenzene was 0.1 g dm^{-3}

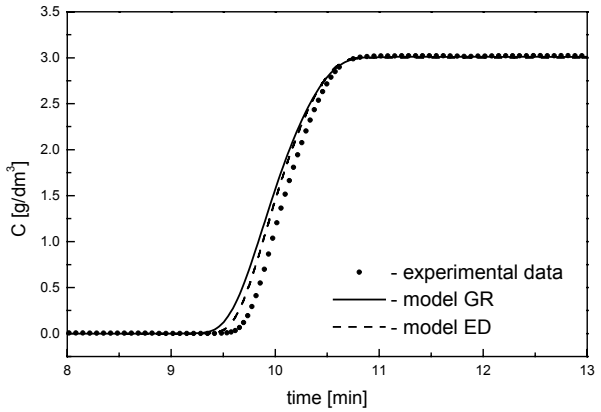

Fig. 7

Comparison of experimental data with theoretical breakthrough profiles calculated by use of the GR and ED models. The inlet concentration of amylbenzene was 3 g dm^{-3}

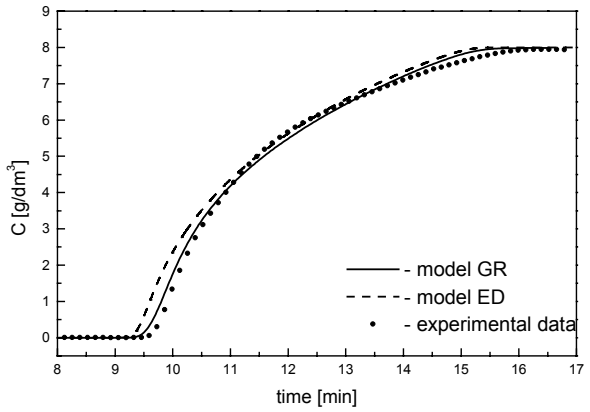

Fig. 8

Comparison of experimental data with theoretical breakthrough profiles calculated by use of the GR and ED models. The inlet concentration of amylbenzene was 8 g dm^{-3}

REFERENCES

[1] G. Guiochon, S.G. Shirazi, and A. Katti, Fundamentals of Preparative and Nonlinear Chromatography, Academic Press, Boston, MA, 1994

[2] M. Diack and G. Guiochon, Anal. Chem., **63**, 2608 (1991)

[3] J.-X. Huang and C. Horvath, J. Chromatogr. A, **406**, 275 (1987)

[4] A. Seidel-Morgenstern and G. Guiochon, Chem. Eng. Sci., **48**, 2787 (1993)

[5] K. Mihlbachler, K. Kaczmarski, A. Seidel – Morgenstern, and G. Guiochon, J. Chromatogr. A, **955**, 35 (2002)

[6] R.H. Fowler and E.A. Guggenheim, Statistical Thermodynamics, Cambridge University Press, Cambridge, UK, 1960

[7] I. Quinones and G. Guiochon, J. Chromatogr. A, **796**, 15 (1998)

[8] A. Cavazzini, G. Bardin, K. Kaczmarski, P. Szabelski, M. Al-Bokari, and G. Guiochon, J. Chromatogr. A, **957**, 111 (2002)

[9] F. Gritti, W. Piątkowski, and G. Guiochon, J. Chromatogr. A, **978**, 81 (2002)

[10] F. Gritti, W. Piątkowski, and G. Guiochon, J. Chromatogr. A, **983**, 51 (2003)

[11] W. Piątkowski, F. Gritti, K. Kaczmarski, and G. Guiochon, J. Chromatogr. A, in press
[12] D.M. Ruthven, Principles of Adsorption and Adsorption Processes, Wiley, New York, 1984
[13] M. Suzuki, Adsorption Engineering, Elsevier, Amsterdam, 1990
[14] V.J. Villadsen and M.L. Michelsen, Solution of Differential Equation Model by Polynomial Approximation, Prentice–Hall, Englewood Cliffs, NJ, 1978
[15] A.J. Berninger, R.D. Whitley, X. Zhang, and N.-H.L. Wang, Comput. Chem. Eng., **15**, 749 (1991)
[16] K. Kaczmarski, G. Storti, M. Mazzotti, and M. Morbidelli, Comput. Chem. Eng., **21**, 641 (1997)
[17] P.N. Brown, A.C. Hindmarsh, and G.D. Byrne, Procedure available from: http://www.netlib.org
[18] G.I. Berezin and A.V. Kiselev, J. Colloid Interface Sci., **38**, 227 (1972)
[19] G.I. Berezin, A.V. Kiselev, and R.T. Sagatelyan, J. Colloid Interface Sci., **38**, 335 (1972)
[20] I. Quinones and G. Guiochon, Langmuir, **12**, 5433 (1996)
[21] S. Brunauer, P.H. Emmet, and E. Teller, J. Am. Chem. Soc., **60**, 309 (1938)
[22] R. Fletcher, A Modified Marquardt Sub-routine for Non-linear Least Squares, AERE-R6788-Harwell
[23] D. Gunn, J. Chem. Eng. Sci., **42**, 363 (1987)
[24] C.R. Wilke and P. Chang, AIChE J., **1**, 264 (1955)
[25] L.R. Perkins and C.J. Geankopolis, Chem. Eng. Sci., **24**, 1035 (1969)
[26] E.J. Wilson and C.J. Geankopolis, Ind. Eng. Chem. Fund., **5**, 9 (1966)